Radical formation by fine particulate matter associated with highly oxygenated molecules

Tong, Haijie; Zhang, Yun; Filippi, Alexander; Wang, Ting; Li, Chenpei; Liu, Fobang; Leppla, Denis ; Kourtchev, Ivan; Wang, Kai; Keskinen, Helmi-Marja; Levula, Janne T.; Arangio, Andrea M.; Shen, Fangxia; Ditas, Florian; Martin, Scot T; Artaxo, P.; Godoi, Ricardo H. M. ; Yamamoto, Carlos. I; de Souza, Rodrigo A. F. ; Huang, Ru-Jin

DOI:
10.1021/acs.est.9b05149

Document Version
Peer reviewed version

Citation for published version (Harvard):
Tong, H, Zhang, Y, Filippi, A, Wang, T, Li, C, Liu, F, Leppla, D, Kourtchev, I, Wang, K, Keskinen, H-M, Levula, JT, Arangio, AM, Shen, F, Ditas, F, Martin, ST, Artaxo, P, Godoi, RHM, Yamamoto, CI, de Souza, RAF, Huang, R-J, Berkemeier, T, Wang, Y, Hang, S, Cheng, Y, Pope, F, Fu, P, Yao, M, Pohlker, C, Petaja, T, Kulmala, M, Andreae, M, Shiraiwa, M, Poschl, U, Hoffmann, T & Markus, K 2019, 'Radical formation by fine particulate matter associated with highly oxygenated molecules', *Environmental Science and Technology*, vol. 53, no. 21, pp. 12506-12518. https://doi.org/10.1021/acs.est.9b05149

Radical Formation by Fine Particulate Matter Associated with Highly Oxygenated Molecules

Haijie Tong,[*1] Yun Zhang,[2] Alexander Filippi,[1] Ting Wang,[1,3] Chenpei Li,[1,3] Fobang Liu,[1,4] Denis Leppla,[2] Ivan Kourtchev,[5] Kai Wang,[2,a] Helmi-Marja Keskinen,[6] Janne T. Levula,[6] Andrea M. Arangio,[1,7] Fangxia Shen,[8] Florian Ditas,[1] Scot T. Martin,[9,10] Paulo Artaxo,[11] Ricardo H. M. Godoi,[12] Carlos I. Yamamoto,[13] Rodrigo A. F. de Souza,[14] Ru-Jin Huang,[15] Thomas Berkemeier,[1] Yueshe Wang,[3] Hang Su,[1] Yafang Cheng,[1] Francis D. Pope,[16] Pingqing Fu,[17] Maosheng Yao,[18] Christopher Pöhlker,[1] Tuukka Petäjä,[6] Markku Kulmala,[6] Meinrat O. Andreae,[1,19] Manabu Shiraiwa,[20] Ulrich Pöschl,[1] Thorsten Hoffmann,[*2] and Markus Kalberer[*5,21]

[1] Multiphase Chemistry Department, Max Planck Institute for Chemistry, 55128 Mainz, Germany.
[2] Institute of Inorganic and Analytical Chemistry, Johannes Gutenberg University, 55128 Mainz, Germany.
[3] State Key Laboratory of Multiphase Flow in Power Engineering, Xi'an Jiaotong University, Xi'an, 710049, China.
[4] School of Chemical and Biomolecular Engineering, Georgia Institute of Technology, Atlanta, Georgia 30332, United States.
[5] Centre for Atmospheric Science, Department of Chemistry, University of Cambridge, Cambridge CB2 1EW, United Kingdom.
[6] Institute for Atmospheric and Earth System Research / Physics Faculty of Science, University of Helsinki FI-00014, Finland.
[7] École polytechnique fédérale de Lausanne, Lausanne 1015, Switzerland.
[8] School of Space and Environment, Beihang University, Beijing, 100191, China.
[9] School of Engineering and Applied Sciences, Harvard University, Cambridge, Massachusetts 02138, United State.
[10] Department of Earth and Planetary Sciences, Harvard University, Cambridge, Massachusetts 02138, United State.
[11] Physics Institute, University of Sao Paulo, Sao Paulo, Brazil.
[12] Environmental Engineering Department, Federal University of Parana, Curitiba, Brazil.
[13] Chemical Engineering Department, Federal University of Parana, Curitiba, PR, Brazil.
[14] State University of Amazonas, Av. Darcy Vergas, 1200, 69065-020, Manaus-AM, Brazil.

[15] Key Laboratory of Aerosol Chemistry and Physics, State Key Laboratory of Loess and Quaternary Geology, Institute of Earth and Environment, Chinese Academy of Sciences, Xi'an, 710061, China.
[16] School of Geography, Earth and Environmental Sciences, University of Birmingham, Birmingham, B15 2TT, United Kingdom.
[17] Institute of Surface-Earth System Science, Tianjin University, Tianjin 300072, China.
[18] College of Environmental Sciences and Engineering, Peking University, Beijing, 100871, China.
[19] Scripps Institution of Oceanography, University of California San Diego, CA 92093, United States.
[20] Department of Chemistry, University of California, Irvine, California 92697-2025, United States.
[21] Department of Environmental Sciences, University of Basel, Klingelbergstrasse 27, 4056 Basel, Switzerland.
[a] now at: Department of Chemistry, Aarhus University, Langelandsgade 140, DK-8000 Aarhus C, Denmark.

ABSTRACT

Highly oxygenated molecules (HOMs) play an important role in the formation and evolution of secondary organic aerosols (SOA). However, the abundance of HOMs in different environments and their relation to the oxidative potential of fine particulate matter (PM) are largely unknown. Here, we investigated the relative HOM abundance and radical yield of laboratory-generated SOA and fine PM in ambient air ranging from remote forest areas to highly polluted megacities. By electron paramagnetic resonance and mass spectrometric investigations, we found that the relative abundance of HOMs especially the dimer and low volatile types in ambient fine PM was positively correlated with the formation of radicals in aqueous PM extracts. SOA from photooxidation of isoprene, ozonolysis of α- and β-pinene as well as fine PM from tropical (central Amazon) and boreal (Hyytiälä, Finland) forests exhibited a higher HOM abundance and radical yield than SOA from photooxidation of naphthalene and fine PM from urban sites (Beijing, Guangzhou, Mainz, Shanghai, and Xi'an), confirming that HOMs are important constituents of biogenic SOA to generate radicals. Our study provides new insights into the chemical relationship of HOM abundance, composition, and sources with the yield of radicals by laboratory and ambient aerosols, enabling better quantification of component-specific contribution of source- or site-specific fine PM to its climate and health effects.

1. INTRODUCTION

Secondary organic aerosols (SOA) account for a major fraction of fine particulate matter ($PM_{2.5}$),[1] which plays a key role in climate change and public health.[2-7] Insights into the chemical and redox characteristics of SOA are important for properly understanding the role of fine PM at the atmosphere-biosphere interface.[8] SOA particles contain a large fraction of reactive substances such as peroxides and highly oxygenated molecules (HOMs).[9-12] The HOMs exist in the gas[12-15] and particle phases[16-21] and they increase the oxidation state and initial growth of organic aerosols, as well as influencing the stability and reactivity of fine PM upon redox chemistry including radical reactions.[12, 20, 22-24] Therefore, a comprehensive understanding of the physicochemical properties of HOMs and their relationship with the oxidative potential of fine PM is challenging but vital to unravel the climate and health effect of SOA.[24]

To date, a few studies have explored the formation mechanism, structure, and chemical aging processes of particle phase HOMs. For instance, gas phase oxidation of organic compounds including Criegee intermediates has been found as efficient formation pathway of HOMs.[13, 16, 20, 25-27] Therein, SOA-bound HOMs were suggested to contain multiple functional groups including hydroperoxides and to have molecular formulae with high atom ratio of oxygen-to-carbon (>0.6 or 0.7).[11-13, 16, 28-30] To subdivide HOMs into different types, HOMs with carbon oxidation state[31] ($\overline{OS_C} \approx 2 \cdot \frac{O}{C} - \frac{H}{C}$) ≥ 0 were assigned to be both highly oxygenated and highly oxidized compounds, while HOMs with $\overline{OS_C} < 0$ were attributed to be highly oxygenated but less oxidized.[16] Furthermore, HOMs in fresh biogenic SOA were found to have formulae more closely resembling low-volatile oxygenated organic aerosols (LV-OOA) than HOMs in aged SOA.[16] Tröstl et al.[11] and Ehn et al.[12] found

87 that HOMs in laboratory-generated α-pinene SOA fell into the following chemical compo-
88 sition range of $C_xH_yO_z$: monomers with x = 8-10, y = 12-16 and z = 6-12, and dimers with
89 x = 17-20, y = 26-32 and z = 8-18.[12, 32] Beyond this, it has been assumed that organic
90 peroxides in α- and β-pinene SOA have molecular weights of < 300 g mol^{-1},[33] falling in the
91 typical molecular weight range of HOM monomers.[12] These peroxides are redox active[11]
92 and can generate reactive species such as radicals through Fenton-like reactions,[23, 34] and
93 photolytic or hydrolytic decomposition in water.[23, 35-37] The reactive species are ubiquitous
94 in atmospheric, environmental, and biological processes exerting strong impacts on climate
95 change and public health.[38, 39] In addition to organic peroxides, high-molecular weight di-
96 mer esters have been found as major products in aerosols from cyclohexene and α-pinene
97 ozonolysis and boreal forest.[40-42] Therefore, HOMs have different sources, complicated
98 composition, and various redox activities. Beyond these findings, the volatility, reactivity,
99 and fate of different source HOMs remain unclear.[24] Insights into these uncertainties will
100 enable a better assessment of aerosol climate and health effects.
101 In this study, HOMs from all laboratory and ambient samples were defined by molecular
102 formula matching the criteria from Tröstl et al.[11] filtering out HOM monomers with *O/C*
103 ratio < 0.7.[16] Based on this criterium, we investigated the relative HOM abundance and
104 radical yield of laboratory SOA formed in a chamber and ambient fine PM in the air rang-
105 ing from remote forests to highly polluted megacities. The correlation of radical yield of
106 fine PM in water with relative fraction of HOMs (RF_{HOM}) among organic constituents was
107 investigated. The RF_{HOM} was defined as the ratio of the number of HOMs ions to all for-
108 mulas identified in a spectrum. The molecular composition of organic aerosol components
109 was determined using an ultra-high-resolution mass spectrometer,[43, 44] and the radicals in

water were identified and quantified using continuous wave electron paramagnetic resonance spectrometry in combination with a spin trapping technique.[36]

2. MATERIALS AND METHODS

2.1 Ambient Particle Sampling. Ambient particles were collected at seven different locations: central Amazon, Hyytiälä, Mainz, Beijing, Shanghai, Guangzhou, and Xi'an. Detailed information on sampling time and instrumentation can be found in Table S1.

The central Amazon fine PM was collected at two different stations. One set of samples was collected from the site 'T3' of GoAmazon2014/5 located in a pasture area that was 70 km west and downwind of Manaus, Amazonas State, Brazil.[45] These samples were used for analyzing the RF_{HOM}. The other set of samples was collected at the Amazon Tall Tower Observatory (ATTO) station, which is located in a remote area of the central Amazon Basin, about 150 km northeast (upwind) of the city of Manaus.[46] At the T3 site, a Harvard impactor (Air Diagnostics, Harrison, ME, USA) and polycarbonate filters (Ø 47 mm, Nuclepore) and were used for PM collection at an air flow of ~10 L min^{-1}. Particles were collected in the dry and wet seasons in 2014 (Table S1). The collected particle samples were stored in a -20 or -80 °C freezer until analysis. At the ATTO site, a micro-orifice uniform deposition impactor (MOUDI, model 125R, MSP corporation, USA) collected sample air from 60 m high inlet at a 80-m tall tower with an air flow rate of ~10 L min^{-1}. Afterwards, the filters were transported from ATTO to Mainz in an ice box and then stored in a -80 °C freezer before analysis. Dry season ATTO PM samples were collected from 20 to 21 October 2017 and 25 to 31 October 2018. These samples were used for analyzing the relationship between ion number and chromatographic peak area indicated relative abundance of HOMs. Wet season samples were collected from 27 March to 25 April 2017.

These samples were used for analyzing the radical yield of PM. More information about the ATTO tower and the typical characteristics of aerosol particles in the upper troposphere over the Amazon Basin can be found in previous studies.[46, 47]

The Hyytiälä fine PM samples were collected from the boreal forest site SMEAR II in Finland from 7 July to 4 August 2014 and from 31 May to 19 July 2017. Scots pine and Norway spruce are the dominant type of trees surrounding the station.[48] A three-stage Dekati PM_{10} impactor together with 47 mm diameter quartz fiber (Pallflex Tissuquartz 2500QAT-UP) and Teflon filters (PALL, Teflon) were used for particle sampling. The quartz filters were pre-baked at 600 °C for half a day to remove organics. The air flow rate through the sampler was ~35 L min^{-1}. After collection, all filter samples were stored at -20 °C before analysis.

The Mainz $PM_{2.5}$ samples were collected onto borosilicate glass fiber filters (Ø 70 mm, Pallflex T60A20, Pall Life Science, USA) using a $PM_{2.5}$ low volume air sampler in January 2015 at the campus site of Johannes Gutenberg University of Mainz. Additional fine MP samples were collected onto 47 mm diameter Teflon filters (100 nm pore size, Merck Chemicals GmbH) on the roof of the Max Planck Institute for Chemistry with a micro-orifice uniform deposition impactor (MOUDI, 110-R, MSP Corporation). The samplings were conducted from August to November 2017 and from March to April 2018. The air flow rate through both samplers was ~30 L min^{-1}. The collected filter samples were stored in -20 °C (samples collected in 2015) or -80 °C (samples collected in 2017 and 2018) freezers before analysis. More information about the aerosol sampling and chemical characteristization can be found in our recent studies.[49, 50]

$PM_{2.5}$ samples in urban site of Beijing,[49] Shanghai, and Guangzhou were collected onto prebaked quartz-fiber filters (8 × 10 inch) in the period between 1 and 23 January 2014 using a high volume air sampler (Tisch, Cleveland, OH, USA) at a flow rate of ~1050 L min^{-1}. Additional $PM_{2.5}$ samples were collected at Peking University campus, central urban region of Beijing, onto 47 mm diameter Teflon filters (100 nm pore size, Merck Chemicals GmbH) in 2016 and 2017 with a TH-16 sampler (Tianhong company, China) at an air flow of ~30 L min^{-1}. The samples collected in 2014 and 2018 were stored in -20 or -80 °C freezers before analysis.

The Xi'an fine PM samples were collected using a low-pressure cascade impactor (Tisch TE-20-800, USA) on the roof of Xi'an Jiaotong University in China. The cut-off aerodynamic diameters of the sampler are 0.43, 0.65, 1.1, 2.1, 3.3, 4.7, 5.8, and 9 μm. Particles were collected onto 90 mm diameter Teflon filters (100 nm pore size, Omnipore JVWP09025, Millipore). Each particle filter sample was collected for 48 h in the period between 14 and 22 September 2017. Before sampling, each filter was cleaned, dried, and weighed.[50] After sampling, filters were stored in a -80 °C freezer before analysis.

2.2 Laboratory SOA Formation and Collection. To compare the relative HOM abundance in anthropogenic and biogenic SOA, we measured the RF_{HOM} in SOA formed from the oxidation of naphthalene, isoprene, and α-pinene, which were used as SOA precursors representative for Beijing,[51] Amazon,[52] and Hyytiälä,[53] respectively. Laboratory SOA was generated in a 7 L quartz flow tube and a laboratory-scale reaction chamber (33 L).[23] α-pinene SOA particles were generated through gas-phase ozonolysis. The isoprene and naphthalene SOA were generated through gas-phase photooxidation by •OH radicals. For the generation of SOA, the O_3 concentration was adjusted in the range of 600-1100 ppb to

generate α-pinene SOA. The •OH concentrations were estimated to be ~5.0×10^{11} cm^{-3} for the formation of isoprene and naphthalene SOA.[36] Based on a calibration function measured by gas chromatography-mass spectrometry, the precursor concentration was estimated to be in the range of 1-2 ppm for α-pinene and 0.5-1 ppm for isoprene and naphthalene. A scanning mobility particle sizer (SMPS, GRIMM Aerosol Technik GmbH & Co. KG) was used to characterize the number and size distribution of SOA particles, which were collected onto 47 mm diameter Teflon filters (JVWP04700, Omnipore membrane filter) and extracted into water immediately after sampling. More information about the SOA formation, characterization, and collection are described in previous studies.[23, 34, 36]

2.3 Ultra-High-Resolution Mass Spectrometer Measurements and Data Processing. The chemical composition of organics in the Amazon and Hyytiälä 2014 fine PM samples were identified using a negative ion mode electrospray ionization (ESI) LTQ Orbitrap mass spectrometer (Thermo Fisher Scientific, MA, USA) at the University of Cambridge. All other filter samples were analyzed at the Johannes Gutenberg University of Mainz, using a Q-Exactive Orbitrap MS (Thermo Fisher Scientific, MA, USA) operated in both negative and positive ion mode ESI and coupled with an ultra-high performance liquid chromatography (UHPLC) system (Dionex UltiMate 3000, Thermo Scientific, Germany). A Hypersil Gold column (C18, 50 × 2.0 mm, 1.9 μm particle size, Thermo Fisher Scientific, MA, USA) was used for analyte separation. Eluent A (ultrapure water with 2% acetonitrile and 0.04% formic acid) and eluent B (acetonitrile with 2% ultrapure water) were used in gradient mode with a flow rate of 500 μL min^{-1}. Detailed information on the optimized gradient can be found in our recent study.[49] Both mass spectrometers were optimized, calibrated

and tuned using chemical standard kits. The filter extraction and data processing methods are the same as we used for organic aerosol composition analysis in previous studies.[49, 54]

After obtaining the MS spectrum and UHPLC chromatogram of one sample, we processed the data through a non-target screening approach by using the commercially available software SIEVE® (Thermo Fisher Scientific, MA, USA).[49] Briefly, we searched the ions with peak abundance > 1×10^5 first, then subtracted the background signals and assigned molecular formulae. The number of C, H, O, N, S, and Cl atoms was constrained to be: 1-39, 1-72, 0-20, 0-7, 0-4, and 0-2 with a tolerance of ± 2 ppm. Furthermore, the atom limits of H/C (0.3-3), O/C (0-3), N/C (0-1.3), S/C (0-0.8), and Cl/C (0-0.8) were used to eliminate chemically unreasonable formulae.

2.4 Continuous Wave Electron Paramagnetic Resonance Measurements. Continuous wave electron paramagnetic resonance (EMXplus-10/12, Bruker, Germany) spectrometry in combination with spin trapping techniques was used to detect radicals. 5-*tert*-Butoxycarbonyl-5-methyl-1-pyrroline-N-oxide (BMPO, high purity, Enzo Life Sciences GmbH) was used as spin trapping agent.[55] The concentration of BMPO in all extracts was 10 mM. The aqueous PM mass concentration in the extracts of ambient fine PM and laboratory SOA was in the range of 250-6300 μg mL^{-1}, with higher concentration for ambient fine PM and lower concentration for laboratory SOA. The aqueous PM mass concentration is defined here as the total PM mass on the filter cut divided by the volume of extraction solvent. The EPR parameters used in this study were the same as in our previous studies.[23, 34, 50] A modulation frequency of 100 kHz, a modulation amplitude of 1, microwave power of 2.1 mW (20 dB), a receiver gain of 40 dB, a time constant of 0.01 ms, a scan number of 50, and a

magnetic field scan of 100 G. The spin fitting and counting methods embedded in the Bruker software, Xenon, were applied for quantification of radicals.[56]

3. RESULTS AND DISCUSSION

3.1 Spectral Fingerprint of HOMs. We distinguished HOMs from other organic components in ambient fine PM from Beijing, Amazon, Hyytiälä, and laboratory SOA from oxidation of α-pinene, isoprene, and naphthalene. We found that ion number fraction of HOMs is in linear positive correlation with the fraction of chromatographic peak area of HOMs averaged from measured samples (Figure S1a, $y=2.37 + 0.70 \times x$, $R^2=0.88$), with the latter one showing positive exponential correlation with radical yield of PM (Figure S1b, $y=0.10 + 0.016 \times \exp(0.37 \times x)$, $R^2=0.99$), indicating that RF_{HOM} may be an indicator of the relative abundance of particle-phase HOMs. Therefore, we showed the mass spectra as well RF of HOMs in Figures 1 and S2.

In ambient samples, most HOMs have been found in remote samples dominated by biogenic SOA, while almost no HOMs found in fine PM in polluted urban sites. The lack of peaks meeting the HOM criteria in Figure 1a indicates that HOMs account for only a little fraction of organic components in Beijing fine PM, with a relative fraction of ~1%. In contrast to Beijing fine PM, fine particles in remote forest air of the Amazon and Hyytiälä have much higher RF_{HOM} of ~4% (Figure 1b) and ~13% (Figure 1c), respectively. This finding agrees well with previous studies, reporting that HOMs and high-molecular weight dimer esters are major components of fine PM from a measurement site in an agricultural pasture area in Germany (Melpitz, Leibniz Institute for Tropospheric Research (TROPOS)) and Hyytiälä, respectively.[20, 41] Thus, ambient particle-phase HOMs are enriched in organic aerosols related to biogenic sources.

As shown in Figure 1d-1f, naphthalene SOA has the lowest RF_{HOM} of ~3% (Figure 1d). In contrast, relative more HOM molecules were observed in isoprene (~7%, Figure 1e) and α-pinene SOA (~14%, Figure 1f). The higher RF_{HOM} of α-pinene SOA than naphthalene SOA agrees with previous studies,[57, 58] and the lower RF_{HOM} of naphthalene SOA may relate to the lower molar yield of extremely low volatile organic compounds (ELVOC) or HOMs from oxidation of naphthalene (~1.8%) compared with α-pinene SOA (~3.4%).[19] In addition, it has been estimated that organic peroxides contributed up to 49%, 85%, 61%, and 28% of α-pinene, β-pinene, isoprene, and naphthalene SOA mass, respectively.[33, 36, 59, 60] The consistent lower abundance of organic peroxides and HOMs in naphthalene SOA than in isoprene, α- and β-pinene SOA may reflect that organic peroxides are one type of HOMs. Finally, the order of RF_{HOM} in the laboratory experiments with naphthalene, isoprene, and α-pinene SOA (Figure 1d-1f) is consistent with ambient fine PM from Beijing, Amazon, and Hyytiälä (Figure 1a-1c), confirming that oxidation of biogenic volatile organic compounds including their autoxidation chemistry, is an efficient formation pathway of ambient particle-phase HOMs.[27] To demonstrate the source dependence of RF_{HOM}, it is useful to clarify the chemical composition and volatility of fine PM-bound HOMs in air ranging from clean background to heavily polluted areas.

3.2 Chemical Composition of Particle Phase HOMs. As shown in Figure 2a, HOM products only composed of carbon, hydrogen, and oxygen (CHO) were preferentially found in laboratory SOA, which was due to the extremely low concentration of NO_x during the experiments. In contrast, ambient fine PM contained relatively little pure CHO compounds as HOMs, however, increasing with the decrease of air pollution levels from Beijing

(~0.4%) to Hyytiälä (~5.1%). In addition to CHO, ambient fine PM also contained substantial fractions of CHON, CHOS, and CHONS forms of HOMs, with higher RF in cleaner air. The RF of CHOS and CHONS forms of HOMs in Amazon and Hyytiälä fine PM accounted for ~2% of total assigned formula, which is comparable to previous findings of organosulfates contributing 4-30% of aerosol mass in central Amazonia,[61] Hungary, and the southeastern U.S.[47, 62, 63] Furthermore, we have observed a synchronous increase of the concentration of NO_x and nitrogen containing organic compounds at Hyytiälä,[64] which might reflect the important role of NO_3-related multigenerational chemistry in organonitrate aerosol formation.[65, 66] Beyond this, Table S2 shows that the RF of the total CHOS subgroup in Shanghai fine PM was ~23%, while the HOMs only account for ~0.4% (Figure 2a). Such a result is in line with previous findings that the major CHOS compounds in Shanghai organic aerosols were organosulfates, which possess distinctive characteristics of long aliphatic carbon chains and a low degree of oxidation.[67, 68]

In this study, all HOMs were assumed to have the same signal response when we compared their peak areas among different samples. However, different organic compounds might have different sensitivity in the mass spectrometer in different ionization modes. Thus, uncertainties exist when comparing the peak areas of HOMs in PM from different sources. To investigate the impact of ion mode on the RF_{HOM}, we compared the RF_{HOM} of different type of PM measured in positive and negative ion modes in Table S3. It was found that 63-93% of particle-phase HOMs were detected in negative mode. This finding is in agreement with the study by Tu et al., which found much more HOMs in laboratory-generated limonene, α- and β-pinene SOA using a quadrupole-orbitrap mass spectrometer coupled with a negative ion mode ESI probe.[16] Thus, the HOMs detected in negative ESI mode

dominate the total HOMs in PM. Furthermore, due to the complexity of the elemental composition of HOMs, more insights into their structural characteristics will enable a better understanding of the connection of different type of HOMs to the oxidative potential of organic aerosols.

3.3 Volatility of Particle-Phase HOMs. The volatility of HOMs in fine PM from different sources was estimated using recently developed parameterization procedure for the volatility of organic compounds.[69] As shown by Figure 2b, laboratory biogenic SOA contained higher RF of highly oxygenated low volatile and extremely low volatile organic compounds (LVOC and ELVOC types of HOMs) compared to ambient fine PM, which contained less LVOC and ELVOC types of HOMs. In addition, the ELVOC type of HOMs were not found in isoprene SOA, which may correlate with the low SOA yield of isoprene and the remarkably low molar yield of gas-phase ELVOC.[57] Furthermore, both LVOC and ELVOC were not found in Shanghai particulate HOMs, an observation that agrees with a previous finding of semi-volatile organic compounds and LVOC as dominant component of CHO subgroup in Shanghai winter fine PM.[68] The RF trend in the ambient samples of LVOC and ELVOC types of HOMs in Figure 2b resembles CHO form of HOMs in Figure 2a, likely reflecting that particle phase HOMs are mainly low volatile CHO species. The generally higher RF of LVOC and ELVOC types of HOMs in the CHOS and CHONS subgroups (Figure S3) indicates that atmospheric nitrogen or sulfur chemistry of particulate HOMs may decrease the volatility and change the oxidative characteristics of organic aerosols.

3.4 HOM Monomers and Dimers in fine PM. Figure 2c showed the RF of HOM monomers and dimers in ambient fine PM and laboratory SOA. The HOM monomers were found

in all analysed particle samples, whereas HOM dimers were only found in fine PM from lightly polluted urban air (Mainz), remote forest air (Amazon and Hyytiälä), and laboratory SOA from α- and β-pinene. The absence of HOM dimers in isoprene-derived SOA may be due to the high volatility of products during the photochemical oxidation of isoprene precursor in the chamber.[57] The relative fraction of dimers in all PM samples increased in the order of polluted urban fine PM<remote forest fine PM<monoterpene SOA, which resembles the trend of RF_{HOM}. The α- and β-pinene SOA were mainly composed of HOM dimers, with RF of ~12% and ~9%, supporting previous findings of high-molecular weight dimer esters as major products in aerosols from α-pinene ozonolysis and boreal forest.[40, 41] Krapf et al. found that peroxide-containing HOMs have half-lives shorter than 1 hr under dark conditions and are thermodynamically unstable.[11] Thus, the extremely low relative fraction of particle phase HOM dimers in urban air may relate to the chemical aging and decomposition of HOMs in ambient fine PM. Furthermore, chemical aging of HOMs via redox chemistry of NO_x or sulfur oxides may change the composition and physicochemical properties of particle phase HOMs in urban fine PM. For example, recent studies have shown that atmospheric sulfur chemistry of HOMs[70] and reactive nitrogen chemistry in aerosol water[71] can be sources of organic and inorganic sulfates, respectively. Finally, it has been found that NO_x chemistry could alter the abundance of organic peroxides in laboratory SOA.[59, 60] This might be a reason for the low abundance of HOM dimers in urban PM, because the HOMs always contain multiple peroxide functionalities.[17]

3.5 Oxidation State of HOMs. Both *O/C* ratio and oxidation state of carbon ($\overline{OS_C}$) were used to describe the oxidation degree of HOMs,[31] where the $\overline{OS_C} = -\sum_i OS_i \frac{n_i}{n_C}$ and the OS_i is the oxidation state associated with element *i*, and the n_i/n_C is the molar ratio of element

336 *i* to carbon. We found that Beijing HOM monomers (Figure 3a) had an *O/C* ratio of 0.89,
337 which is lower than Amazon HOM monomers (0.95) but higher than Hyytiälä monomers
338 (0.88). Such a trend is inconsistent with the RF of HOMs and may not reflect the oxidation
339 state of organic aerosols properly. Therefore, we plotted the *O/C* and *H/C* ratios of HOMs
340 as well as $\overline{OS_C}$ for different values in Figure 3. To obtain $\overline{OS_C}$, we assumed the oxidation
341 state of *N* and *S* to be +5 and +6 respectively. We found that the oxidation state of carbon
342 in HOM monomers in fine PM from Beijing (-0.11, Figure 3a) is on average lower than in
343 the Amazon (-0.06, black circles in Figure 3b) and Hyytiälä (0.21, black circles in Figure
344 3c). This may relate to the stronger contribution of alkane derivatives from gasoline and
345 lubrication oil vapors from anthropogenic emissions in Beijing.[72] Furthermore, Beijing fine
346 PM contained amounts of HOM dimers below the detection limit (Figure 2c), whereas
347 Amazon and Hyytiälä fine PM contained a large fraction of HOM dimers (pink circles in
348 Figure 3b and 3c) exhibiting typical $\overline{OS_C}$ between -1.0 (red dotted line) and 0.0 (blue dot-
349 ted line), with average values of -0.64 and -0.59, respectively. Therefore, the oxidation
350 state and RF of HOMs (Figure 2c) in Beijing, Amazon, and Hyytiälä were observed in the
351 same range, however, with higher values for the cleaner sites.
352 To compare the oxidation state characteristics of HOMs in anthropogenic and biogenic
353 SOA, Figure 3d-3f show the *O/C* and *H/C* ratios of laboratory-generated naphthalene, iso-
354 prene, and α-pinene SOA as well as the $\overline{OS_C}$ lines. We found that the HOM monomers in
355 naphthalene SOA had a larger *O/C* ratio (1.06) than biogenic SOA (isoprene: 0.90, and α-
356 pinene: 0.78), and the $\overline{OS_C}$ of HOM monomers in naphthalene SOA (0.73) is also higher
357 than in isoprene (0.14) and α-pinene SOA (-0.65), which is different from the lower $\overline{OS_C}$
358 of HOM monomers in Beijing fine PM than in Amazon and Hyytiälä fine PM. This may

be due to the different chemical aging processes of ambient fine PM from laboratory SOA, e.g., the absence of NO_x- and SO_2-related chemistry in our chamber experiments. Finally, ~20%, ~43%, and ~62% of the HOMs in Beijing (Figure 3a), Amazon (Figure 3b), and Hyytiälä (Figure 3c) fine PM had an oxidation state between -1.0 and 0.0. Similarly, none, ~19%, and ~91% of the HOMs in naphthalene (Figure 3d), isoprene (Figure 3e), and α-pinene SOA (Figure 3f) had the same range of oxidation states. This consistency indicates that highly oxygenated but less oxidized HOMs should determine the oxidative potential of ambient fine PM and laboratory SOA.[16]

3.6 Yield and Formation Potential of Radicals by Ambient fine PM. To characterize the reactive species formation potential of ambient fine PM, we measured the radical yield and radical formation potential of fine PM from different sources in water. The results are shown in Figures 4, 5, and S4. Figure 4a displays the EPR spectra of BMPO-radical adducts formed in fine PM water extracts with BMPO. The multiple peaks in the spectra indicate the formation of different radicals. Individual peaks were assigned to adducts of $^{\bullet}OH$, $O_2^{\bullet-}$, C- and O-centered radicals, respectively. Figure 4b shows the relative fraction of formed radicals ($RF_{radical}$), and the amount of individual radicals quantified based on spin-fitting and -counting techniques.[36] The fine PM from highly polluted megacities such as Shanghai, Guangzhou, and Beijing mainly generated $^{\bullet}OH$ and $O_2^{\bullet-}$ radicals, whereas the fine PM from less polluted urban and remote forest sites of Mainz, Amazon, and Hyytiälä dominantly yielded organic radicals. The higher yield of $^{\bullet}OH$ and $O_2^{\bullet-}$ by fine PM from highly polluted megacities may be related to the enhanced Fenton-like reactions associated with higher abundance of water-soluble transition metals.[73] The lower $^{\bullet}OH$ but higher organic radical

yield of fine PM from the Amazon and Hyytiälä may be due to Fenton-like reactions initiated by transition metals and relatively stable organic hydroperoxides,[23, 35, 36] and also the interaction of •OH with SOA material.[74]

Beyond the $RF_{radical}$, the radical yield from a given mass of particles or the formation potential in a given volume of air can also reflect radical formation of fine PM. Figure 5a shows that the sample-volume-normalized radical formation potential of ambient fine PM has a positive linear correlation with $PM_{2.5}$ concentration ($R^2 = 0.85$): $y = 1.47 + 0.11 \times x$. Shanghai fine PM exhibited the highest formation potential of ~15 pmol m^{-3} radicals in ~96 μg m^{-3} $PM_{2.5}$, whereas ~3.5 μg m^{-3} Amazon $PM_{2.5}$ generated only ~3 pmol m^{-3} radicals. Thus, the radical formation potential of fine PM may become a metric reflecting the relative health risk of different concentrations of fine PM in air ranging from clean background to heavily polluted areas. As indicated in Figure 3, the oxidation state of HOMs in fine PM from remote forests (Amazon and Hyytiälä) and laboratory α-pinene SOA was mainly in the range of -1.0-1.0. Thus, we assume that radical formation by organic aerosols in water was mainly driven by highly oxygenated but less oxidized HOMs,[16] which had molecular formulae similar to low-volatile oxygenated organic aerosols.[16, 75] Figure 5b shows the aerosol-sample-mass-normalized total radical yield of ambient fine PM, which shows a negative power-law correlation with $PM_{2.5}$ concentrations ($R^2 = 0.90$): $y = x^{-0.43}$. Specifically, the Hyytiälä fine PM had the highest radical yield of ~0.7 pmol μg^{-1}, while the fine PM from Xi'an, Beijing, Guangzhou, and Shanghai generated only 0.1-0.2 pmol μg^{-1} radicals. The trend of higher radical yield from fine PM at remote forest sites compared to urban sites resembles the organic radical yield in Figure 4b and Figure S4 as well as the RF_{HOM}

403 in Figure 2, supporting the conclusion that HOMs represent important source for radicals,
404 especially organic radicals in water.

405 A previous study showed that at -20 °C, the concentration of peroxides in α-pinene SOA
406 decreased < 20% in one week.[35] In this study, the laboratory SOA were collected immedi-
407 ately after their formation and analyzed within 4 hours. Thus, the influence of aging effects
408 on the relative HOM abundance and radical yield of laboratory SOA is negligible. Regard-
409 ing the ambient PM samples, their RF_{HOM} and radical yield were measured within a few
410 days. Therefore, particle aging should not influence the relationship of RF_{HOM} and radical
411 yield in Figure 6 significantly.

412 **3.7 Association of RF_{HOM} with Radical Yield.** As shown in Figure 6 and S1b, both radical
413 yields of ambient fine PM ($y=0.071 + 0.015 \times \exp(0.44 \times x)$, $R^2 = 0.74$) and laboratory
414 SOA ($y=1.8 + 0.011 \times \exp(0.52 \times x)$, $R^2 = 0.92$) showed positive exponential correlations
415 with the RF_{HOM} and chromatographic peak area fraction of HOMs, with the laboratory
416 SOA showing a higher radical yield. This may reflect the different redox activity of HOMs
417 in ambient fine PM and laboratory SOA. The larger deviations of radical yield and RF_{HOM}
418 of Amazon and Hyytiälä fine PM than urban fine PM may be due to the seasonal or year-
419 to-year aerosol composition variations due to changing meteorological conditions.[43, 64, 76]
420 In contrast to ambient fine PM, laboratory SOA had much higher radical yield. Among
421 laboratory SOA, β-pinene SOA had the highest RF_{HOM} of ~11.5% and radical yield of ~5.9
422 pmol μg^{-1}, whereas naphthalene SOA had the lowest RF_{HOM} of ~3.3% and radical yield of
423 ~1.8 pmol μg^{-1}. Isoprene and α-pinene SOA exhibited similar RF_{HOM} of ~10.4% and
424 ~10.0%, and radical yields of ~4.5 and ~3.4 pmol μg^{-1}. The higher radical yield of labora-
425 tory SOA may mainly be due to the higher relative fraction of CHO forms of HOMs in

426 fresh laboratory SOA (Figure 3b). The consistent positive exponential correlations of
427 RF_{HOM} and radical yield of ambient fine PM and laboratory SOA strongly indicate that
428 HOMs are closely associated with the radical formation by PM in water.

429 To explore the influence of ionization mode during mass spectrometry analysis on the
430 association of radical yield by PM with RF_{HOM}, we show the Spearman correlation coeffi-
431 cients (r) of radical yields (pmol μg^{-1}) with chemical groups analyzed in negative mode,
432 positive mode, and their sum in Table S4. It can be seen that radical yield has close corre-
433 lation with RF of total HOMs, HOM dimer, and LVOC type of HOMs identified in the
434 different modes. Therefore, Tables S3 and S4 indicate that RF_{HOM} measured in negative
435 mode resembles the distribution of total HOMs in fine PM.

436 To explore the association of different types of HOMs with the radical yield, we calcu-
437 lated the Spearman correlation matrix[77] of total HOMs and individual chemical subgroups
438 with the aerosol-sample-mass-normalized radical yield (Figure 7 and Table S4, method see
439 SI). As shown in Figure 7, blue colors and negative values indicate negative correlations,
440 and red colors and positive values indicate positive correlations. When Spearman r is ≥0,
441 lighter color represents weaker correlation, vice versa for negative Spearman r. The relative
442 fraction of total HOMs showed one of the strongest correlations with the yield of total
443 radicals (Spearman r = 0.92), confirming the important role of HOMs in generating radi-
444 cals. Moreover, the CHO forms of HOMs showed close positive correlation with the total
445 radical yield (Spearman r = 0.91). In contrast, the CHON form of HOMs showed much
446 weaker correlation with total radical yield (Spearman r = 0.13). Furthermore, both CHOS
447 and CHONS forms of HOMs had negative correlations with the radical yield (Spearman r
448 = -0.30 and -0.35). Therefore, the CHO forms of HOMs may play stronger roles than

449 CHON, CHOS, and CHONS forms of HOMs in radical formation, and atmospheric chem-
450 istry of nitrogen or sulfur should decrease the radical yield of organic aerosols in water.
451 This can be explained by the decreased abundance of organic hydroperoxides upon for-
452 mation of organic nitrates.[66, 78, 79] In addition to the CHO form of HOMs, the highly oxy-
453 genated SVOC and LVOC subgroups also showed close correlation with total radical yield
454 (Spearman r = 0.56 and 0.95), which is in line with the lower RF of ELVOCs in the CHO
455 form of HOMs (Figure S3). Furthermore, the HOM dimers showed a closer correlation
456 with the total radical yield of fine PM (Spearman r=0.94), reflecting an important role of
457 HOM dimers in generating radicals. This is consistent with previous findings of higher
458 oxidation potential of oligomer-rich fractions of SOA from polycyclic aromatic hydrocar-
459 bons.[80] In contrast, the HOM monomers had weak correlation with the radical yield (Spear-
460 man r=0.23), indicating that HOM monomers may decompose and lost more efficiently
461 during particle aging. This hypothesis is supported by the finding of Krapf et al., which
462 demonstrated that organic peroxides in α-pinene SOA are thermodynamically unstable
463 with half-lives shorter than 1 hr under dark conditions.[11] In addition, other studies also
464 found that organic peroxides including organic hydroperoxides might be involved in the
465 formation of organosulfates,[20] oligomers,[81] and radicals in water.[23, 34-36] Therefore, organic
466 peroxides may undergo heterogeneous chemical reactions during atmospheric aging pro-
467 cesses. Given the presence of peroxide functional groups in HOMs, we speculate that the
468 weak correlation of HOM monomers with the radical yield of fine PM from different
469 sources may be due to aging processes of particle-phase HOMs. Furthermore, organic-
470 metal interactions have shown synergistic effects in producing reactive oxygen species.[80,
471 82] Thus, we suggest that the close correlation of RF_{HOM} with radical formation may also

relate to redox chemistry involving metal ions. Finally, Table S4 and Figure S5 indicate that radical yields of ambient fine PM and laboratory SOA have a weak negative correlation with the *O/C* ratio (Spearman r=-0.42) and oxidation state ($\overline{OS_C}$) (Spearman r = -0.3) of totally assigned compounds, supporting the conclusion of highly oxygenated but less oxidized HOMs as important radical precursor of fine PM in water.

In conclusion, we found that HOMs are closely associated with the radical formation by ambient fine PM and laboratory-generated SOA in water. The formed radicals may influence the formation and evolution of SOA through multigenerational chemical processes.[8, 24, 83-86] For example, aqueous-phase chemistry of HOMs has been suggested to be a major pathway for the formation of organosulfates.[70, 87] In addition, HOMs are suggested to contain at least one, and often multiple, hydroperoxide, peroxide, or peroxy acid groups.[24] These reactive functional groups may initiate redox chemistry including Fenton-like reactions,[23, 28, 35, 74, 88-90] which may change the reactivity and role of fine PM during atmospheric processing. Beyond their climate effects, HOMs may exert adverse health effects due to the enrichment of organic peroxides and their ability to generate reactive species. For instance, exposure of lung epithelial cells to photochemically aged SOA showed increased toxic effects, which may relate to the elevated abundance of peroxides in aged SOA.[88] Thus, our findings may provide new insights in quantifying the contribution of specific components to climate and health effects of fine PM from different sources.[91] Considering that HOMs widely exist in both biogenic and anthropogenic organic aerosols, the seasonality dependence and physicochemical properties of HOMs from different sources and their exact role in environmental and biological processes need to be investigated. Fi-

494 nally, during the ESI-MS measurement, ion suppression, ion enhancement, solvent inter-
495 action, and adduct formation etc. may influence the HOM detectability or the sensitivity of
496 the method in distinguishing different type of HOMs, which warrants follow-up studies.

ASSOCIATED CONTENT

Supporting Information

Supporting material consists of three tables and four figures.

AUTHOR INFORMATION

Corresponding Author

*E-mail: h.tong@mpic.de. Tel: +4961313057040.

*E-mail: hoffmant@uni-mainz.de. Tel: +4961313925716.

*E-mail: markus.kalberer@unibas.ch. Tel: +41612070701.

ORCID

Haijie Tong: 0000-0001-9887-7836

Maosheng Yao: 0000-0002-1442-8054

Christopher Pöhlker: 0000-0001-6958-425X

Meinrat O. Andreae: 0000-0003-1968-7925

Manabu Shiraiwa: 0000-0003-2532-5373

Ulrich Pöschl: 0000-0003-1412-3557

Notes

The authors declare no competing financial interest.

ACKNOWLEDGEMENT

519 This work was funded by the Max Planck Society, National Science Fund for Distinguished
520 Young Scholars (41625014), Projects of International Cooperation and Exchanges NSFC
521 (projects no. 41571130024 and 51576160), ACTRIS, ECAC, the Finnish Centre of Excel-
522 lence under Academy of Finland (projects no. 307331 and 272041), German Federal Min-
523 istry of Edu-cation and Research (BMBF contracts 01LB1001A and 01LK1602B), Brazil-
524 ian Ministério da Ciência, Tecnologia e Inovação (MCTI/FINEP contract 01.11.01248.00),
525 China Scholarship Council, and Deutscher Akademischer Austauschdienst (DAAD). Tech-
526 nical staffs at the SMEARII station are acknowledged for logistical support during sample
527 collection. For the operation of the ATTO site, we acknowledge the support by the Amazon
528 State University (UEA), FAPEAM, the Central Office of the Large Scale Biosphere At-
529 mosphere Experiment in Amazonia (LBA), the National Institute of Amazonian Research
530 (INPA), and SDS/CEUC/RDS-Uatumã. This paper contains results of research conducted
531 under the Technical/Scientific Cooperation Agreement between the National Institute for
532 Amazonian Research, the State University of Amazonas, and the Max-Planck-Gesellschaft
533 e.V.; the opinions expressed are the entire responsibility of the authors and not of the par-
534 ticipating institutions. For the operation of the T3 site, institutional support was provided
535 by the Central Office of LBA, INPA, and UEA. We acknowledge support from the Atmos-
536 pheric Radiation Measurement (ARM) Climate Research Facility, a user facility of the
537 United States Department of Energy (DOE, DE-SC0006680), Office of Science, sponsored
538 by the Office of Biological and Environmental Research. The research was conducted un-
539 der scientific license 001030/2012-4 of the Brazilian National Council for Scientific and
540 Technological Development (CNPq). MS acknowledges funding from U.S. National Sci-
541 ence Foundation (CHE-1808125).
542

REFERENCES

1. Hallquist, M.; Wenger, J.; Baltensperger, U.; Rudich, Y.; Simpson, D.; Claeys, M.; Dommen, J.; Donahue, N.; George, C.; Goldstein, A.; Hamilton, J. F.; Herrmann, H.; Hoffmann, T.; Iinuma, Y.; Jang, M.; Jenkin, M. E.; Jimenez, J. L.; Kiendler-Scharr, A.; Maenhaut, W.; McFiggans, G.; Mentel, T. F.; Monod, A.; Prévôt, A. S. H.; Seinfeld, J. H.; Surratt, J. D.; Szmigielski, R.; Wildt, J. The formation, properties and impact of secondary organic aerosol: current and emerging issues. *Atmos. Chem. Phys.* **2009**, *9* (14), 5155-5236.
2. Shrivastava, M.; Cappa, C. D.; Fan, J.; Goldstein, A. H.; Guenther, A. B.; Jimenez, J. L.; Kuang, C.; Laskin, A.; Martin, S. T.; Ng, N. L.; Cappa, C. D.; Jimenez, J. L.; Seinfeld, J. H.; Volkamer, R.; Fan, J.; Smith, J. N.; Petaja, T.; Pierce, J. R.; Rasch, P. J.; Shilling, J.; Goldstein, A. H.; Kuang, C.; Laskin, A.; Thornton, J. A.; Wang, J.; Worsnop, D. R.; Zaveri, R. A.; Roldin, P.; Zelenyuk, A.; Zhang, Q. Recent advances in understanding secondary organic aerosol: Implications for global climate forcing. *Rev. Geophys.* **2017**, *55* (2), 509-559.
3. West, J. J.; Cohen, A.; Dentener, F.; Brunekreef, B.; Zhu, T.; Armstrong, B.; Bell, M. L.; Brauer, M.; Carmichael, G.; Costa, D. L.; Dockery, D. W.; Kleeman, M.; Krzyzanowski, M.; Künzli, N.; Liousse, C.; Candice Lung, S.-C.; Martin, R. V.; Pöschl, U.; Pope, C. A.; Roberts, J. M.; Russell, A. G.; Wiedinmyer, C. What we breathe impacts our health: improving understanding of the link between air pollution and health. *Environ. Sci. Technol.* **2016**, *50*, 4895-4904.
4. Shiraiwa, M.; Ueda, K.; Pozzer, A.; Lammel, G.; Kampf, C. J.; Fushimi, A.; Enami, S.; Arangio, A. M.; Fröhlich-Nowoisky, J.; Fujitani, Y.; Furuyama, A.; Furuyama, A.; Lakey, P. S. J.; Lelieveld, J.; Lucas, K.; Morino, Y.; Pöschl, U.; Takahama, S.; Takami, A.; Tong, H.; Weber, B.; Yoshino, A.; Sato, K. Aerosol health effects from molecular to global scales. *Environ. Sci. Technol.* **2017**, *51* (23), 13545-13567.
5. Lelieveld, J.; Poschl, U. Chemists can help to solve the air-pollution health crisis. *Nature* **2017**, *551* (7680), 291-293.
6. Lelieveld, J.; Klingmüller, K.; Pozzer, A.; Pöschl, U.; Fnais, M.; Daiber, A.; Münzel, T. Cardiovascular disease burden from ambient air pollution in Europe reassessed using novel hazard ratio functions. *Eur. Heart J.* **2019**, *40* (20), 1590-1596.
7. Lelieveld, J.; Klingmüller, K.; Pozzer, A.; Burnett, R.; Haines, A.; Ramanathan, V. Effects of fossil fuel and total anthropogenic emission removal on public health and climate. *Proc. Natl. Acad. Sci. U. S. A.* **2019**, *116*, 7192-7197.
8. Pöschl, U.; Shiraiwa, M. Multiphase chemistry at the atmosphere–biosphere interface influencing climate and public health in the anthropocene. *Chem. Rev.* **2015**, *115* (10), 4440-4475.
9. Noziere, B.; Kalberer, M.; Claeys, M.; Allan, J.; D'Anna, B.; Decesari, S.; Finessi, E.; Glasius, M.; Grgic, I.; Hamilton, J. F.; Hoffmann, T.; Iinuma, Y.; Jaoui, M.; Kahnt, A.; Kampf, C. J.; Kourtchev, I.; Maenhaut, W.; Marsden, N.; Saarikoski, S.; Schnelle-Kreis, J. r.; Surratt, J. D.; Szidat, S. n.; Szmigielski, R.; Wisthaler, A. The molecular identification of organic compounds in the atmosphere: state of the art and challenges. *Chem. Rev.* **2015**, *115* (10), 3919-3983.
10. Liu, P.; Li, Y. J.; Wang, Y.; Gilles, M. K.; Zaveri, R. A.; Bertram, A. K.; Martin, S. T. Lability of secondary organic particulate matter. *Proc. Natl. Acad. Sci. U. S. A.* **2016**, *113* (45), 12643-12648.
11. Krapf, M.; El Haddad, I.; Bruns, E. A.; Molteni, U.; Daellenbach, K. R.; Prévôt, A. S.; Baltensperger, U.; Dommen, J. Labile peroxides in secondary organic aerosol. *Chem* **2016**, *1* (4), 603-616.
12. Tröstl, J.; Chuang, W. K.; Gordon, H.; Heinritzi, M.; Yan, C.; Molteni, U.; Ahlm, L.; Frege, C.; Bianchi, F.; Wagner, R.; Simon, M.; Lehtipalo, K.; Williamson, C.; Craven, J. S.; Duplissy, J.; Adamov, A.; Almeida, J.; Bernhammer, A.-K.; Breitenlechner, M.; Brilke, S.; Dias, A.; Ehrhart, S.; Flagan, R. C.; Franchin, A.; Fuchs, C.; Guida, R.; Gysel, M.; Hansel, A.; Hoyle, C. R.; Jokinen, T.; Junninen, H.; Kangasluoma, J.; Keskinen, H.; Kim, J.; Krapf, M.; Kürten, A.; Laaksonen, A.; Lawler, M.; Leiminger, M.; Mathot, S.; Möhler, O.; Nieminen, T.; Onnela, A.; Petäjä, T.; Piel, F. M.; Miettinen, P.; Rissanen, M. P.; Rondo, L.; Sarnela, N.; Schobesberger, S.; Sengupta, K.; Sipilä,

M.; Smith, J. N.; Steiner, G.; Tomè, A.; Virtanen, A.; Wagner, A. C.; Weingartner, E.; Wimmer, D.; Winkler, P. M.; Ye, P.; Carslaw, K. S.; Curtius, J.; Dommen, J.; Kirkby, J.; Kulmala, M.; Riipinen, I.; Worsnop, D. R.; Donahue, N. M.; Baltensperger, U. The role of low-volatility organic compounds in initial particle growth in the atmosphere. *Nature* **2016**, *533* (7604), 527-531.
13. Ehn, M.; Kleist, E.; Junninen, H.; Petäjä, T.; Lönn, G.; Schobesberger, S.; Maso, M. D.; Trimborn, A.; Kulmala, M.; Worsnop, D. R.; Wahner, A.; Wildt, J.; Mentel, T. F. Gas phase formation of extremely oxidized pinene reaction products in chamber and ambient air. *Atmos. Chem. Phys.* **2012**, *12* (11), 5113-5127.
14. Bianchi, F.; Garmash, O.; He, X.; Yan, C.; Iyer, S.; Rosendahl, I.; Xu, Z.; Rissanen, M. P.; Riva, M.; Taipale, R.; Sarnela, N.; Tuukka Petäjä; Worsnop, D. R.; Kulmala, M.; Ehn, M.; Junninen, H. The role of highly oxygenated molecules (HOMs) in determining the composition of ambient ions in the boreal forest. *Atmos. Chem. Phys.* **2017**, *17* (22), 13819-13831.
15. Wang, Z.; Popolan-Vaida, D. M.; Chen, B.; Moshammer, K.; Mohamed, S. Y.; Wang, H.; Sioud, S.; Raji, M. A.; Kohse-Höinghaus, K.; Hansen, N.; Dagaut, P.; Leone, S. R.; Sarathy, S. M. Unraveling the structure and chemical mechanisms of highly oxygenated intermediates in oxidation of organic compounds. *Proc. Natl. Acad. Sci. U. S. A.* **2017**, *114* (50), 13102–13107.
16. Tu, P.; Hall IV, W. A.; Johnston, M. V. Characterization of highly oxidized molecules in fresh and aged biogenic secondary organic aerosol. *Anal. Chem.* **2016**, *88* (8), 4495-4501.
17. Zhang, X.; Lambe, A. T.; Upshur, M. A.; Brooks, W. A.; Gray Bé, A.; Thomson, R. J.; Geiger, F. M.; Surratt, J. D.; Zhang, Z.; Gold, A.; Graf, S.; Cubison, M. J.; Groessl, M.; Jayne, J. T.; Worsnop, D. R.; Canagaratna, M. R. Highly oxygenated multifunctional compounds in α-pinene secondary organic aerosol. *Environ. Sci. Technol.* **2017**, *51* (11), 5932-5940.
18. Lee, B. H.; Lopez-Hilfiker, F. D.; D'Ambro, E. L.; Zhou, P.; Boy, M.; Petäjä, T.; Hao, L.; Virtanen, A.; Thornton, J. A. Semi-volatile and highly oxygenated gaseous and particulate organic compounds observed above a boreal forest canopy. *Atmos. Chem. Phys.* **2018**, *18* (15), 11547-11562.
19. Molteni, U.; Bianchi, F.; Klein, F.; Haddad, I. E.; Frege, C.; Rossi, M. J.; Dommen, J.; Baltensperger, U. Formation of highly oxygenated organic molecules from aromatic compounds. *Atmos. Chem. Phys.* **2018**, *18* (3), 1909-1921.
20. Mutzel, A.; Poulain, L.; Berndt, T.; Iinuma, Y.; Rodigast, M.; Böge, O.; Richters, S.; Spindler, G.; Sipilä, M.; Jokinen, T.; Kulmala, M.; Herrmann, H. Highly oxidized multifunctional organic compounds observed in tropospheric particles: A field and laboratory study. *Environ. Sci. Technol.* **2015**, *49* (13), 7754-7761.
21. Zhang, X.; McVay, R. C.; Huang, D. D.; Dalleska, N. F.; Aumont, B.; Flagan, R. C.; Seinfeld, J. H. Formation and evolution of molecular products in α-pinene secondary organic aerosol. *Proc. Natl. Acad. Sci. U. S. A.* **2015**, *112* (46), 14168-14173.
22. Kirkby, J.; Duplissy, J.; Sengupta, K.; Frege, C.; Gordon, H.; Williamson, C.; Heinritzi, M.; Simon, M.; Yan, C.; Almeida, J.; Tröstl, J.; Nieminen, T.; Ortega, I. K.; Wagner, R.; Adamov, A.; Amorim, A.; Bernhammer, A.-K.; Bianchi, F.; Breitenlechner, M.; Brilke, S.; Chen, X.; Craven, J.; Dias, A.; Ehrhart, S.; Flagan, R. C.; Franchin, A.; Fuchs, C.; Guida, R.; Hakala, J.; Hoyle, C. R.; Jokinen, T.; Junninen, H.; Kangasluoma, J.; Kim, J.; Krapf, M.; Kürten, A.; Laaksonen, A.; Lehtipalo, K.; Makhmutov, V.; Mathot, S.; Molteni, U.; Onnela, A.; Peräkylä, O.; Piel, F.; Petäjä, T.; Praplan, A. P.; Pringle, K.; Rap, A.; Richards, N. A. D.; Riipinen, I.; Rissanen, M. P.; Rondo, L.; Sarnela, N.; Schobesberger, S.; Scott, C. E.; Seinfeld, J. H.; Sipilä, M.; Steiner, G.; Stozhkov, Y.; Stratmann, F.; Tomé, A.; Virtanen, A.; Vogel, A. L.; Wagner, A. C.; Wagner, P. E.; Weingartner, E.; Wimmer, D.; Winkler, P. M.; Ye, P.; Zhang, X.; Hansel, A.; Dommen, J.; Donahue, N. M.; Worsnop, D. R.; Baltensperger, U.; Kulmala, M.; Carslaw, K. S.; Curtius, J. Ion-induced nucleation of pure biogenic particles. *Nature* **2016**, *533*, 521-526.
23. Tong, H.; Arangio, A. M.; Lakey, P. S.; Berkemeier, T.; Liu, F.; Kampf, C. J.; Brune, W. H.; Pöschl, U.; Shiraiwa, M. Hydroxyl radicals from secondary organic aerosol decomposition in water. *Atmos. Chem. Phys.* **2016**, *16* (3), 1761-1771.

24. Bianchi, F.; Kurtén, T.; Riva, M.; Mohr, C.; Rissanen, M. P.; Roldin, P.; Berndt, T.; Crounse, J. D.; Wennberg, P. O.; Mentel, T. F.; Wildt, J.; Junninen, H.; Jokinen, T.; Kulmala, M.; Worsnop, D. R.; Thornton, J. A.; Donahue, N.; Kjaergaard, H. G.; Ehn, M. Highly Oxygenated Organic Molecules (HOM) from Gas-Phase Autoxidation Involving Peroxy Radicals: A Key Contributor to Atmospheric Aerosol. *Chem. Rev.* **2019**, *119*, 3472−3509.
25. Crounse, J. D.; Nielsen, L. B.; Jørgensen, S.; Kjaergaard, H. G.; Wennberg, P. O. Autoxidation of organic compounds in the atmosphere. *J. Phys. Chem. Lett.* **2013**, *4* (20), 3513-3520.
26. McGillen, M. R.; Curchod, B. F.; Chhantyal-Pun, R.; Beames, J. M.; Watson, N.; Khan, M. A. H.; McMahon, L.; Shallcross, D. E.; Orr-Ewing, A. J. Criegee Intermediate–Alcohol Reactions, A Potential Source of Functionalized Hydroperoxides in the Atmosphere. *ACS Earth Space Chem.* **2017**, *1* (10), 664-672.
27. Praske, E.; Otkjær, R. V.; Crounse, J. D.; Hethcox, J. C.; Stoltz, B. M.; Kjaergaard, H. G.; Wennberg, P. O. Atmospheric autoxidation is increasingly important in urban and suburban North America. *Proc. Natl. Acad. Sci. U. S. A.* **2018**, *115* (1), 64-69.
28. Riva, M. Multiphase chemistry of highly oxidized molecules: the case of organic hydroperoxides. *Chem* **2016**, *1* (4), 526-528.
29. Epstein, S. A.; Blair, S. L.; Nizkorodov, S. A. Direct photolysis of α-pinene ozonolysis secondary organic aerosol: effect on particle mass and peroxide content. *Environ. Sci. Technol.* **2014**, *48* (19), 11251-11258.
30. Pagonis, D.; Ziemann, P. J. Chemistry of hydroperoxycarbonyls in secondary organic aerosol. *Aerosol Sci. Technol.* **2018**, *52* (10), 1178-1193.
31. Kroll, J. H.; Donahue, N. M.; Jimenez, J. L.; Kessler, S. H.; Canagaratna, M. R.; Wilson, K. R.; Altieri, K. E.; Mazzoleni, L. R.; Wozniak, A. S.; Bluhm, H.; Mysak, E. R.; Smith, J. D.; Kolb, C. E.; Worsnop, D. R. Carbon oxidation state as a metric for describing the chemistry of atmospheric organic aerosol. *Nat. Chem.* **2011**, *3* (2), 133-139.
32. Ehn, M.; Thornton, J. A.; Kleist, E.; Sipilä, M.; Junninen, H.; Pullinen, I.; Springer, M.; Rubach, F.; Tillmann, R.; Lee, B.; Lopez-Hilfiker, F.; Andres, S.; Acir, I.-H.; Rissanen, M.; Jokinen, T.; Schobesberger, S.; Kangasluoma, J.; Kontkanen, J.; Nieminen, T.; Kurtén, T.; Nielsen, L. B.; Jørgensen, S.; Kjaergaard, H. G.; Canagaratna, M. R.; Maso, M. D.; Berndt, T.; Tuukka Petäjä; Wahner, A.; Kerminen, V.-M.; Kulmala, M.; Worsnop, D. R.; Wildt, J.; Mentel, T. F. A large source of low-volatility secondary organic aerosol. *Nature* **2014**, *506* (7489), 476-479.
33. Docherty, K. S.; Wu, W.; Lim, Y. B.; Ziemann, P. J. Contributions of organic peroxides to secondary aerosol formed from reactions of monoterpenes with O3. *Environ. Sci. Technol.* **2005**, *39* (11), 4049-4059.
34. Tong, H.; Lakey, P. S.; Arangio, A. M.; Socorro, J.; Kampf, C. J.; Berkemeier, T.; Brune, W. H.; Pöschl, U.; Shiraiwa, M. Reactive oxygen species formed in aqueous mixtures of secondary organic aerosols and mineral dust influencing cloud chemistry and public health in the Anthropocene. *Faraday Discuss.* **2017**, *200*, 251-270.
35. Badali, K.; Zhou, S.; Aljawhary, D.; Antiñolo, M.; Chen, W.; Lok, A.; Mungall, E.; Wong, J.; Zhao, R.; Abbatt, J. Formation of hydroxyl radicals from photolysis of secondary organic aerosol material. *Atmos. Chem. Phys.*, **2015**, *15* (14), 7831-7840.
36. Tong, H.; Lakey, P. S.; Arangio, A. M.; Socorro, J.; Shen, F.; Lucas, K.; Brune, W. H.; Pöschl, U.; Shiraiwa, M. Reactive Oxygen Species Formed by Secondary Organic Aerosols in Water and Surrogate Lung Fluid. *Environ. Sci. Technol.* **2018**, *52* (20), 11642-11651.
37. Zhao, R.; Aljawhary, D.; Lee, A. K.; Abbatt, J. P. Rapid aqueous-phase photooxidation of dimers in the α-pinene secondary organic aerosol. *Environ. Sci. Technol. Lett.* **2017**, *4* (6), 205-210.
38. Gligorovski, S.; Strekowski, R.; Barbati, S.; Vione, D. Environmental implications of hydroxyl radicals (• OH). *Chem. Rev.* **2015**, *115* (24), 13051-13092.

39. Anglada, J. M.; Martins-Costa, M.; Francisco, J. S.; Ruiz-Lopez, M. F. Interconnection of reactive oxygen species chemistry across the interfaces of atmospheric, environmental, and biological processes. *Acc. Chem. Res.* **2015**, *48* (3), 575-583.
40. Müller, L.; Reinnig, M.-C.; Warnke, J.; Hoffmann, T. Unambiguous identification of esters as oligomers in secondary organic aerosol formed from cyclohexene and cyclohexene/α-pinene ozonolysis. *Atmos. Chem. Phys.* **2008**, *8* (5), 1423-1433.
41. Kristensen, K.; Watne, Å. K.; Hammes, J.; Lutz, A.; Petäjä, T.; Hallquist, M.; Bilde, M.; Glasius, M. High-molecular weight dimer esters are major products in aerosols from α-pinene ozonolysis and the boreal forest. *Environ. Sci. Technol. Lett.* **2016**, *3* (8), 280-285.
42. Kahnt, A.; Vermeylen, R.; Iinuma, Y.; Safi Shalamzari, M.; Maenhaut, W.; Claeys, M. High-molecular-weight esters in α-pinene ozonolysis secondary organic aerosol: structural characterization and mechanistic proposal for their formation from highly oxygenated molecules. *Atmos. Chem. Phys.* **2018**, *18* (11), 8453-8467.
43. Kourtchev, I.; Godoi, R. H.; Connors, S.; Levine, J. G.; Archibald, A. T.; Godoi, A. F.; Paralovo, S. L.; Barbosa, C. G.; Souza, R. A.; Manzi, A. O.; Seco, R.; Sjostedt, S.; Park, J.-H.; Guenther, A.; Kim, S.; Smith, J.; Martin, S. T.; Kalberer, M. Molecular composition of organic aerosols in central Amazonia: an ultra-high-resolution mass spectrometry study. *Atmos. Chem. Phys.* **2016**, *16* (18), 11899-11913.
44. Zielinski, A. T.; Kourtchev, I.; Bortolini, C.; Fuller, S. J.; Giorio, C.; Popoola, O. A.; Bogialli, S.; Tapparo, A.; Jones, R. L.; Kalberer, M. A new processing scheme for ultra-high resolution direct infusion mass spectrometry data. *Atmos. Environ.* **2018**, *178*, 129-139.
45. Martin, S.; Artaxo, P.; Machado, L.; Manzi, A.; Souza, R.; Schumacher, C.; Wang, J.; Andreae, M.; Barbosa, H.; Fan, J.; Fisch, G.; Goldstein, A. H.; Guenther, A.; Jimenez, J. L.; Pöschl, U.; Silva Dias, M. A.; Smith, J. N.; Wendisch, M. Introduction: observations and modeling of the Green Ocean Amazon (GoAmazon2014/5). *Atmos. Chem. Phys.* **2016**, *16* (8), 4785–4797.
46. Andreae, M.; Acevedo, O.; Araùjo, A.; Artaxo, P.; Barbosa, C.; Barbosa, H.; Brito, J.; Carbone, S.; Chi, X.; Cintra, B. B. L.; da Silva, N. F.; Dias, N. L.; Dias-Júnior; F. Ditas, C. Q.; Ditz, R.; Godoi, A. F. L.; Godoi, R. H. M.; Heimann, M.; Hoffmann, T.; Kesselmeier, J.; Könemann, T.; Krüger, M. L.; Lavric, J. V.; Manzi, A. O.; Lopes, A. P.; Martins, D. L.; Mikhailov, E. F.; Moran-Zuloaga, D.; Nelson, B. W.; Nölscher, A. C.; Santos Nogueira, D.; Piedade, M. T. F.; Pöhlker, C.; Pöschl, U.; Quesada, C. A.; Rizzo, L. V.; Ro, C.-U.; Ruckteschler, N.; Sá, L. D. A.; de Oliveira Sá, M.; Sales, C. B.; dos Santos, R. M. N.; Saturno, J.; Schöngart, J.; Sörgel, M.; Souza, C. M. d.; de Souza, R. A. F.; Su, H.; Targhetta, N.; Tóta, J.; Trebs, I.; Trumbore, S.; van Eijck, A.; Walter, D.; Wang, Z.; Weber, B.; Williams, J.; Winderlich, J.; Wittmann, F.; Wolff, S.; Yáñez-Serrano, A. M. The Amazon Tall Tower Observatory (ATTO): overview of pilot measurements on ecosystem ecology, meteorology, trace gases, and aerosols. *Atmos. Chem. Phys.* **2015**, *15* (18), 10723-10776.
47. Andreae, M. O.; Afchine, A.; Albrecht, R.; Holanda, B. A.; Artaxo, P.; Barbosa, H. M.; Borrmann, S.; Cecchini, M. A.; Costa, A.; Dollner, M.; Fütterer, D.; Järvinen, E.; Jurkat, T.; Klimach, T.; Konemann, T.; Knote, C.; Krämer, M.; Krisna, T.; Machado, L. A. T.; Mertes, S.; Minikin, A.; Pöhlker, C.; Pöhlker, M. L.; Pöschl, U.; Rosenfeld, D.; Sauer, D.; Schlager, H.; Schnaiter, M.; Schneider, J.; Schulz, C.; Spanu, A.; Sperling, V. B.; Voigt, C.; Walser, A.; Wang, J.; Weinzierl, B.; Wendisch, M.; Ziereis, H. Aerosol characteristics and particle production in the upper troposphere over the Amazon Basin. *Atmos. Chem. Phys.* **2018**, *18* (2), 921-961.
48. Hari, P.; Kulmala, M. Station for measuring ecosystem-atmosphere relations: SMEAR. *Boreal Environ. Res.* **2005**, *10*, 315-322.
49. Wang, K.; Zhang, Y.; Huang, R.-J.; Cao, J.; Hoffmann, T. UHPLC-Orbitrap mass spectrometric characterization of organic aerosol from a central European city (Mainz, Germany) and a Chinese megacity (Beijing). *Atmos. Environ.* **2018**, *189*, 22-29.

50. Arangio, A. M.; Tong, H.; Socorro, J.; Pöschl, U.; Shiraiwa, M. Quantification of environmentally persistent free radicals and reactive oxygen species in atmospheric aerosol particles. *Atmos. Chem. Phys.* **2016**, *16* (20), 13105-13119.
51. Huang, G.; Liu, Y.; Shao, M.; Li, Y.; Chen, Q.; Zheng, Y.; Wu, Z.; Liu, Y.; Wu, Y.; Hu, M.; Li, X.; Lu, S.; Wang, C.; Liu, J.; Zheng, M.; Zhu, T. Potentially Important Contribution of Gas-Phase Oxidation of Naphthalene and Methylnaphthalene to Secondary Organic Aerosol during Haze Events in Beijing. *Environ. Sci. Technol.* **2019**, *53* (3), 1235-1244.
52. Liu, Y.; Brito, J.; Dorris, M. R.; Rivera-Rios, J. C.; Seco, R.; Bates, K. H.; Artaxo, P.; Duvoisin, S.; Keutsch, F. N.; Kim, S.; Goldstein, A. H.; Guenther, A. B.; Manzi, A. O.; Souza, R. A. F.; Springston, S. R.; Watson, T. B.; McKinney, K. A.; Martin, S. T. Isoprene photochemistry over the Amazon rainforest. *Proc. Natl. Acad. Sci. U. S. A.* **2016**, *113* (22), 6125-6130.
53. Hakola, H.; Hellén, H.; Hemmilä, M.; Rinne, J.; Kulmala, M. In situ measurements of volatile organic compounds in a boreal forest. *Atmos. Chem. Phys.* **2012**, *12* (23), 11665-11678.
54. Gallimore, P. J.; Mahon, B. M.; Wragg, F. P.; Fuller, S. J.; Giorio, C.; Kourtchev, I.; Kalberer, M. Multiphase composition changes and reactive oxygen species formation during limonene oxidation in the new Cambridge Atmospheric Simulation Chamber (CASC). *Atmos. Chem. Phys.* **2017**, *17* (16), 9853-9868.
55. Zhao, H.; Joseph, J.; Zhang, H.; Karoui, H.; Kalyanaraman, B. Synthesis and biochemical applications of a solid cyclic nitrone spin trap: a relatively superior trap for detecting superoxide anions and glutathiyl radicals. *Free Radical Biol. Med.* **2001**, *31* (5), 599-606.
56. Weber, R. T., *Xenon Data Processing Reference* 2012; Vol. Bruker Instruments: Billerica, MA.
57. Jokinen, T.; Berndt, T.; Makkonen, R.; Kerminen, V.-M.; Junninen, H.; Paasonen, P.; Stratmann, F.; Herrmann, H.; Guenther, A. B.; Worsnop, D. R.; Kulmala, M.; Ehn, M.; Sipilä, M. Production of extremely low volatile organic compounds from biogenic emissions: Measured yields and atmospheric implications. *Proc. Natl. Acad. Sci. U. S. A.* **2015**, *112* (23), 7123–7128.
58. Gatzsche, K.; Iinuma, Y.; Tilgner, A.; Mutzel, A.; Berndt, T.; Wolke, R. Kinetic modeling studies of SOA formation from α-pinene ozonolysis. *Atmos. Chem. Phys.* **2017**, *17* (21), 13187–13211.
59. Surratt, J. D.; Murphy, S. M.; Kroll, J. H.; Ng, N. L.; Hildebrandt, L.; Sorooshian, A.; Szmigielski, R.; Vermeylen, R.; Maenhaut, W.; Claeys, M.; Flagan, R. C.; Seinfeld, J. H. Chemical composition of secondary organic aerosol formed from the photooxidation of isoprene. *J. Phys. Chem. A* **2006**, *110* (31), 9665-9690.
60. Kautzman, K.; Surratt, J.; Chan, M.; Chan, A.; Hersey, S.; Chhabra, P.; Dalleska, N.; Wennberg, P.; Flagan, R.; Seinfeld, J. Chemical composition of gas-and aerosol-phase products from the photooxidation of naphthalene. *J. Phys. Chem. A* **2010**, *114* (2), 913-934.
61. Schulz, C.; Schneider, J.; Holanda, B. A.; Appel, O.; Costa, A.; de Sá, S. S.; Dreiling, V.; Fütterer, D.; Jurkat-Witschas, T.; Klimach, T.; Knote, C.; Krämer, M.; Martin, S. T.; Mertes, S.; Pöhlker, M. L.; Sauer, D.; Voigt, C.; Walser, A.; Weinzierl, B.; Ziereis, H.; Zöger, M.; Andreae, M. O.; Artaxo, P.; Machado, L. A. T.; Pöschl, U.; Wendisch, M.; Borrmann, S. Aircraft-based observations of isoprene-epoxydiol-derived secondary organic aerosol (IEPOX-SOA) in the tropical upper troposphere over the Amazon region. *Atmos. Chem. Phys.* **2018**, *18* (20), 14979-15001.
62. Surratt, J. D.; Gómez-González, Y.; Chan, A. W.; Vermeylen, R.; Shahgholi, M.; Kleindienst, T. E.; Edney, E. O.; Offenberg, J. H.; Lewandowski, M.; Jaoui, M.; Maenhaut, W.; Claeys, M.; Flagan, R. C.; Seinfeld, J. H. Organosulfate formation in biogenic secondary organic aerosol. *J. Phys. Chem. A* **2008**, *112* (36), 8345-8378.
63. Glasius, M.; Bering, M. S.; Yee, L. D.; de Sá, S. S.; Isaacman-VanWertz, G.; Wernis, R. A.; Barbosa, H. M.; Alexander, M. L.; Palm, B. B.; Hu, W.; Campuzano-Jost, P.; Day, D. A.; Jimenez, J. L.; Shrivastava, M.; Martin, S. T.; Goldstein, A. H. Organosulfates in aerosols

794 downwind of an urban region in central Amazon. *Environ. Sci.: Processes Impacts* **2018**, *20* (11),
795 1546-1558.
796 64. Kourtchev, I.; Fuller, S.; Aalto, J.; Ruuskanen, T. M.; McLeod, M. W.; Maenhaut, W.;
797 Jones, R.; Kulmala, M.; Kalberer, M. Molecular composition of boreal forest aerosol from
798 Hyytiala, Finland, using ultrahigh resolution mass spectrometry. *Environ. Sci. Technol.* **2013**, *47*
799 (9), 4069-4079.
800 65. Rollins, A. W.; Browne, E. C.; Min, K.-E.; Pusede, S. E.; Wooldridge, P. J.; Gentner, D.
801 R.; Goldstein, A. H.; Liu, S.; Day, D. A.; Russell, L. M.; Cohen, R. C. Evidence for NOx control
802 over nighttime SOA formation. *Science* **2012**, *337* (6099), 1210-1212.
803 66. Berkemeier, T.; Ammann, M.; Mentel, T. F.; Pöschl, U.; Shiraiwa, M. Organic nitrate
804 contribution to new particle formation and growth in secondary organic aerosols from α-pinene
805 ozonolysis. *Environ. Sci. Technol.* **2016**, *50* (12), 6334-6342.
806 67. Tao, S.; Lu, X.; Levac, N.; Bateman, A. P.; Nguyen, T. B.; Bones, D. L.; Nizkorodov, S.
807 A.; Laskin, J.; Laskin, A.; Yang, X. Molecular characterization of organosulfates in organic
808 aerosols from Shanghai and Los Angeles urban areas by nanospray-desorption electrospray
809 ionization high-resolution mass spectrometry. *Environ. Sci. Technol.* **2014**, *48* (18), 10993-11001.
810 68. Wang, X.; Hayeck, N.; Brüggemann, M.; Yao, L.; Chen, H.; Zhang, C.; Emmelin, C.;
811 Chen, J.; George, C.; Wang, L. Chemical Characteristics of Organic Aerosols in Shanghai: A Study
812 by Ultrahigh‐Performance Liquid Chromatography Coupled With Orbitrap Mass Spectrometry.
813 *J. Geophys. Res* **2017**, *122*, 11703-11722.
814 69. Li, Y.; Pöschl, U.; Shiraiwa, M. Molecular corridors and parameterizations of volatility in
815 the chemical evolution of organic aerosols. *Atmos. Chem. Phys.* **2016**, *16* (5), 3327-3344.
816 70. Hunt, S. W.; Laskin, A.; Nizkorodov, S. A., *Multiphase Environmental Chemistry in the*
817 *Atmosphere*. ACS Symposium Series, American Chemical Society, Washington, DC: 2018.
818 71. Cheng, Y.; Zheng, G.; Wei, C.; Mu, Q.; Zheng, B.; Wang, Z.; Gao, M.; Zhang, Q.; He, K.;
819 Carmichael, G.; Pöschl, U.; Su, H. Reactive nitrogen chemistry in aerosol water as a source of
820 sulfate during haze events in China. *Sci. Adv.* **2016**, *2* (12), e1601530.
821 72. Tang, R.; Wu, Z.; Li, X.; Wang, Y.; Shang, D.; Xiao, Y.; Li, M.; Zeng, L.; Wu, Z.;
822 Hallquist, M.; Hu, M.; Guo, S. Primary and secondary organic aerosols in summer 2016 in Beijing.
823 *Atmos. Chem. Phys.* **2018**, *18* (6), 4055-4068.
824 73. Lakey, P. S.; Berkemeier, T.; Tong, H.; Arangio, A. M.; Lucas, K.; Pöschl, U.; Shiraiwa,
825 M. Chemical exposure-response relationship between air pollutants and reactive oxygen species in
826 the human respiratory tract. *Sci. Rep.* **2016**, *6*, 32916.
827 74. Hems, R. F.; Hsieh, J. S.; Slodki, M. A.; Zhou, S.; Abbatt, J. P. Suppression of OH
828 generation from the Photo-Fenton reaction in the presence of α-Pinene secondary organic aerosol
829 material. *Environ. Sci. Technol. Lett.* **2017**, *4* (10), 439-443.
830 75. Jimenez, J. L.; Canagaratna, M.; Donahue, N.; Prevot, A.; Zhang, Q.; Kroll, J. H.; DeCarlo,
831 P. F.; Allan, J. D.; Coe, H.; Ng, N. L.; Aiken, A. C.; Docherty, K. S.; Ulbrich, I. M.; Grieshop, A.
832 P.; Robinson, A. L.; Duplissy, J.; Smith, J. D.; Wilson, K. R.; Lanz, V. A.; Hueglin, C.; Sun, Y. L.;
833 Tian, J.; Laaksonen, A.; Raatikainen, T.; Rautiainen, J.; Vaattovaara, P.; Ehn, M.; Kulmala, M.;
834 Tomlinson, J. M.; Collins, D. R.; Cubison, M. J.; Dunlea, E. J.; Huffman, J. A.; Onasch, T. B.;
835 Alfarra, M. R.; Williams, P. I.; Bower, K.; Kondo, Y.; J., S.; Drewnick, F.; Borrmann, S.; Weimer,
836 S.; Demerjian, K.; Salcedo, D.; Cottrell, L.; Griffin, R.; Takami, A.; Miyoshi, T.; Hatakeyama, S.;
837 Shimono, A.; Sun, J. Y.; Zhang, Y. M.; Dzepina, K.; Kimmel, J. R.; Sueper, D.; Jayne, J. T.;
838 Herndon, S. C.; Trimborn, A. M.; Williams, L. R.; Wood, E. C.; Middlebrook, A. M.; Kolb, C. E.;
839 Baltensperger, U.; Worsnop, D. R. Evolution of organic aerosols in the atmosphere. *science* **2009**,
840 *326* (5959), 1525-1529.
841 76. Kourtchev, I.; Giorio, C.; Manninen, A.; Wilson, E.; Mahon, B.; Aalto, J.; Kajos, M.;
842 Venables, D.; Ruuskanen, T.; Levula, J.; Loponen, M.; Connors, S.; Harris, N.; Zhao, D.; Kiendler-
843 Scharr, A.; Mentel, T. F.; Rudich, Y.; Hallquist, M.; Doussin, J.-F.; Maenhaut, W.; Bäck, J.; Petäjä,

T.; Wenger, J. C.; Kulmala, M.; Kalberer, M. Enhanced Volatile Organic Compounds emissions and organic aerosol mass increase the oligomer content of atmospheric aerosols. *Sci. Rep.* **2016**, *6*, 35038.
77. Brehmer, C.; Lai, A. M.; Clark, S.; Shan, M.; Ni, K.; Ezzati, M.; Yang, X.; Baumgartner, J.; Schauer, J. J.; Carter, E. The Oxidative Potential of Personal and Household PM2. 5 in a Rural Setting in Southwestern China. *Environ. Sci. Technol.* **2019**, *53*, 2788−2798.
78. Lee, B. H.; Mohr, C.; Lopez-Hilfiker, F. D.; Lutz, A.; Hallquist, M.; Lee, L.; Romer, P.; Cohen, R. C.; Iyer, S.; Kurtén, T.; Weiwei Hu; Douglas A. Day; Pedro Campuzano-Jost; Jimenez, J. L.; Xu, L.; Ng, N. L.; Guo, H.; Weber, R. J.; Wild, R. J.; Brown, S. S.; Koss, A.; Gouw, J. d.; Olson, K.; Goldstein, A. H.; Seco, R.; Kim, S.; McAvey, K.; Shepson, P. B.; Starn, T.; Baumann, K.; Edgerton, E. S.; Liu, J.; Shilling, J. E.; Miller, D. O.; Brune, W. H.; Schobesberger, S.; D'Ambro, E. L.; Thornton, J. A. Highly functionalized organic nitrates in the southeast United States: Contribution to secondary organic aerosol and reactive nitrogen budgets. *Proc. Natl. Acad. Sci. U. S. A.* **2016**, *113* (6), 1516-1521.
79. Ng, N. L.; Brown, S. S.; Archibald, A. T.; Atlas, E.; Cohen, R. C.; Crowley, J. N.; Day, D. A.; Donahue, N. M.; Fry, J. L.; Fuchs, H.; Griffin, R. J.; Guzman, M. I.; Herrmann, H.; Hodzic, A.; Iinuma, Y.; Jimenez, J. L.; Kiendler-Scharr, A.; Lee, B. H.; Luecken, D. J.; Mao, J.; McLaren, R.; Mutzel, A.; Osthoff, H. D.; Ouyang, B.; Picquet-Varrault, B.; Platt, U.; Pye, H. O. T.; Rudich, Y.; Schwantes, R. H.; Shiraiwa, M.; Stutz, J.; Thornton, J. A.; Tilgner, A.; Williams, B. J.; Zaveri, R. A. Nitrate radicals and biogenic volatile organic compounds: oxidation, mechanisms, and organic aerosol. *Atmos. Chem. Phys.* **2017**, *17* (3), 2103-2162.
80. Wang, S.; Ye, J.; Soong, R.; Wu, B.; Yu, L.; Simpson, A. J.; Chan, A. W. Relationship between chemical composition and oxidative potential of secondary organic aerosol from polycyclic aromatic hydrocarbons. *Atmos. Chem. Phys.* **2018**, *18* (6), 3987-4003.
81. Riva, M.; Budisulistiorini, S. H.; Chen, Y.; Zhang, Z.; D'Ambro, E. L.; Zhang, X.; Gold, A.; Turpin, B. J.; Thornton, J. A.; Canagaratna, M. R.; Surratt, J. D. Chemical characterization of secondary organic aerosol from oxidation of isoprene hydroxyhydroperoxides. *Environ. Sci. Technol.* **2016**, *50* (18), 9889-9899.
82. Wei, J.; Yu, H.; Wang, Y.; Verma, V. Complexation of Iron and Copper in Ambient Particulate Matter and Its Effect on the Oxidative Potential Measured in a Surrogate Lung Fluid. *Environ. Sci. Technol.* **2019**, *53* (3), 1661-1671.
83. Ervens, B.; Turpin, B.; Weber, R. Secondary organic aerosol formation in cloud droplets and aqueous particles (aqSOA): a review of laboratory, field and model studies. *Atmos. Chem. Phys.* **2011**, *11* (21), 11069-11102.
84. Herrmann, H.; Schaefer, T.; Tilgner, A.; Styler, S. A.; Weller, C.; Teich, M.; Otto, T. Tropospheric aqueous-phase chemistry: kinetics, mechanisms, and its coupling to a changing gas phase. *Chem. Rev.* **2015**, *115* (10), 4259-4334.
85. Gilardoni, S.; Massoli, P.; Paglione, M.; Giulianelli, L.; Carbone, C.; Rinaldi, M.; Decesari, S.; Sandrini, S.; Costabile, F.; Gobbi, G. P.; Pietrogrande, M. C.; Visentind, M.; Scottoe, F.; Fuzzia, S.; Facchinia, M. C. Direct observation of aqueous secondary organic aerosol from biomass-burning emissions. *Proc. Natl. Acad. Sci. U. S. A.* **2016**, *113* (36), 10013-10018.
86. Riva, M.; Heikkinen, L.; Bell, D.; Peräkylä, O.; Zha, Q.; Schallhart, S.; Rissanen, M.; Imre, D.; Petäjä, T.; Thornton, J. A.; Zelenyuk, A.; Ehn, M. Chemical transformations in monoterpene-derived organic aerosol enhanced by inorganic composition. *npj Clim. Atmos. Sci.* **2019**, *2* (1), 2.
87. Brüggemann, M.; Poulain, L.; Held, A.; Stelzer, T.; Zuth, C.; Richters, S.; Mutzel, A.; Pinxteren, D. v.; Iinuma, Y.; Katkevica, S.; Rabe, R.; Herrmann, H.; Hoffmann, T. Real-time detection of highly oxidized organosulfates and BSOA marker compounds during the F-BEACh 2014 field study. *Atmos. Chem. Phys.* **2017**, *17* (2), 1453-1469.
88. Chowdhury, P. H.; He, Q.; Lasitza Male, T.; Brune, W. H.; Rudich, Y.; Pardo, M. Exposure of Lung Epithelial Cells to Photochemically-Aged Secondary Organic Aerosol Shows Increased Toxic Effects. *Environ. Sci. Technol. Lett.* **2018**, *5*, 424-430.

89. Hua, W.; Chen, Z.; Jie, C.; Kondo, Y.; Hofzumahaus, A.; Takegawa, N.; Chang, C.; Lu, K.; Miyazaki, Y.; Kita, K.; Wang, H. L.; Zhang, Y. H.; Hu, M. Atmospheric hydrogen peroxide and organic hydroperoxides during PRIDE-PRD'06, China: their concentration, formation mechanism and contribution to secondary aerosols. *Atmos. Chem. Phys.* **2008**, *8* (22), 6755-6773.
90. Li, X.; Chee, S.; Hao, J.; Abbatt, J. P.; Jiang, J.; Smith, J. N. Relative humidity effect on the formation of highly oxidized molecules and new particles during monoterpene oxidation. *Atmos. Chem. Phys.* **2019**, *19* (3), 1555-1570.
91. Jin, L.; Xie, J.; Wong, C. K.-C.; Chan, S. K.; Abbaszade, G.; Schnelle-Kreis, J.; Zimmermann, R.; Li, J.; Zhang, G.; Fu, P.; Li, X. Contributions of city-specific PM2. 5 to differential in vitro oxidative stress and toxicity implications between Beijing and Guangzhou of China. *Environ. Sci. Technol.* **2019**, *53*, 2881-2891.

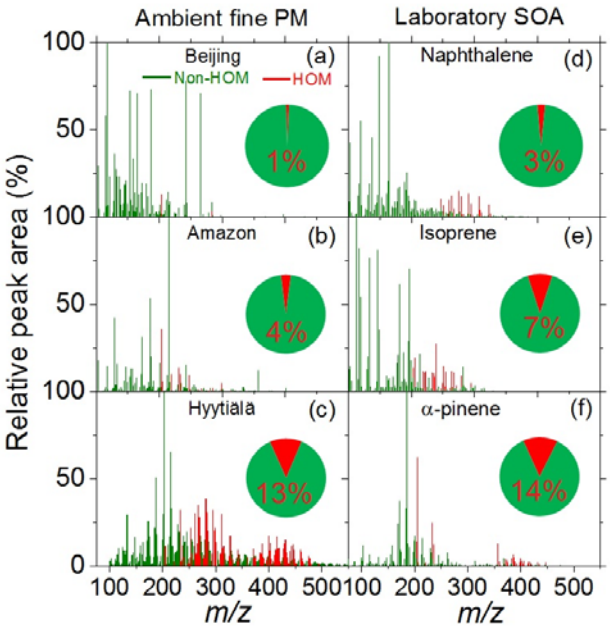

907
908 **Figure 1**. The spectral fingerprint and relative fraction of HOMs (red) and non-HOMs (green) in
909 different type of particles. The mass spectra were measured using LC-MS technique. The chroma-
910 tographic peak areas were used to calculate relative fractions of HOMs for the pie charts. The rel-
911 ative peak area (%) of the spectra belonging to HOMs in ambient PM and laboratory SOA were
912 multiplied by a factor of 3 and 10, respectively. The pie charts and enclosed numbers indicate the
913 ion number fraction of HOMs and non-HOMs. The spectra in panel a-c are for PM samples col-
914 lected in January 2017, October 2018, and July-August 2014.
915

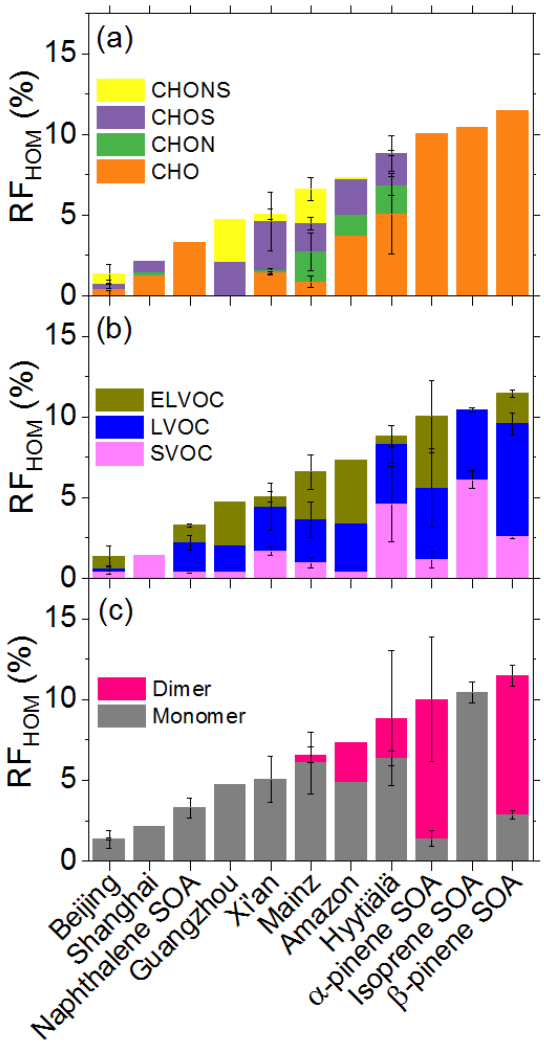

916

917 **Figure 2.** Chemical composition and volatility of HOMs in fine particles from different sources.

918 (a) Chemical composition of HOMs. (b) Relative fractions of HOMs with different volatility. (c)

919 Relative fractions of HOM dimers and monomers. The error bars represent the standard deviations

920 of measurements with more than three individual samples.

921

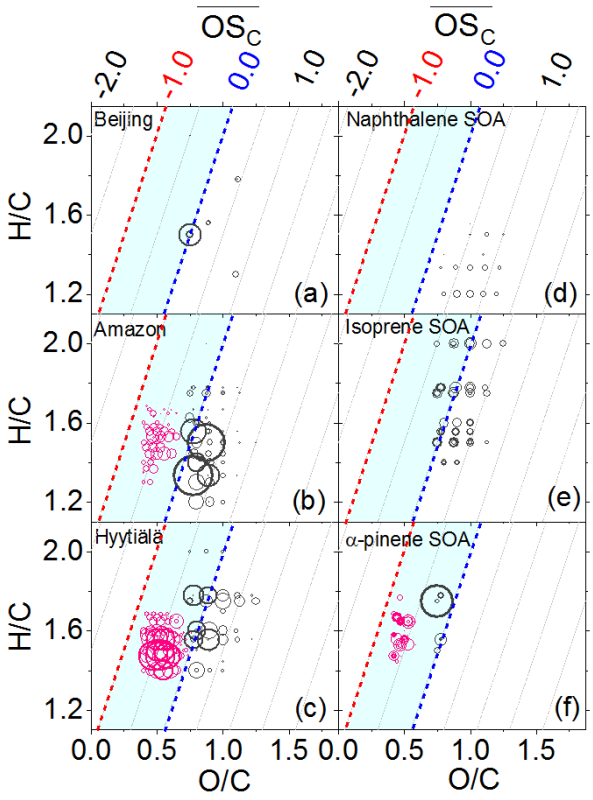

Figure 3. Van Krevelen and oxidation state diagrams for HOMs in fine PM from Beijing (a), Amazon (b), and Hyytiälä (c) as well as in SOA from oxidation of naphthalene (d), isoprene (e), and α-pinene (f). The red and blue dotted lines represent $\overline{OS_C}$ =−1.0 and 0.0, respectively. The cyan shaded areas represent oxidation states ranging from -1.0 to 0.0. Pink and dark grey data points represent HOM dimers and monomers, respectively. The size of the symbols reflects the relative peak intensities in the mass spectra. The scaling factor for Amazon and Hyytiälä monomers is 1 and for other data points it is 3. The results in panel a-c were based on selected fine PM samples collected in November 2017, June 2017, and March-October 2014, respectively.

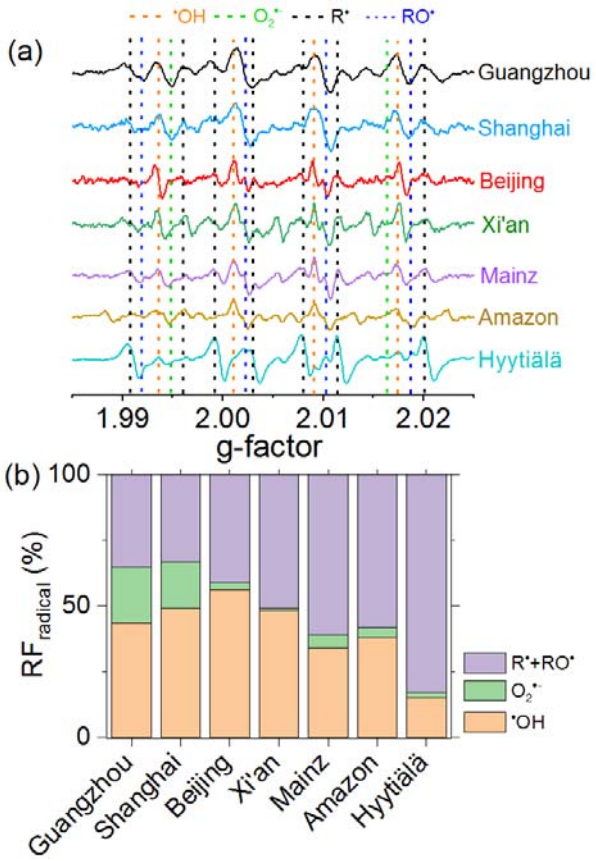

933

934 **Figure 4.** (a) EPR spectra and (b) relative fraction of radicals ($RF_{radical}$) formed by ambient fine

935 particles. The yellow, green, black, and blue dashed lines in panel (a) indicate the peaks assigned

936 to $^{\bullet}OH$, $O_2^{\bullet-}$, C- and O-centered radicals, respectively.

937

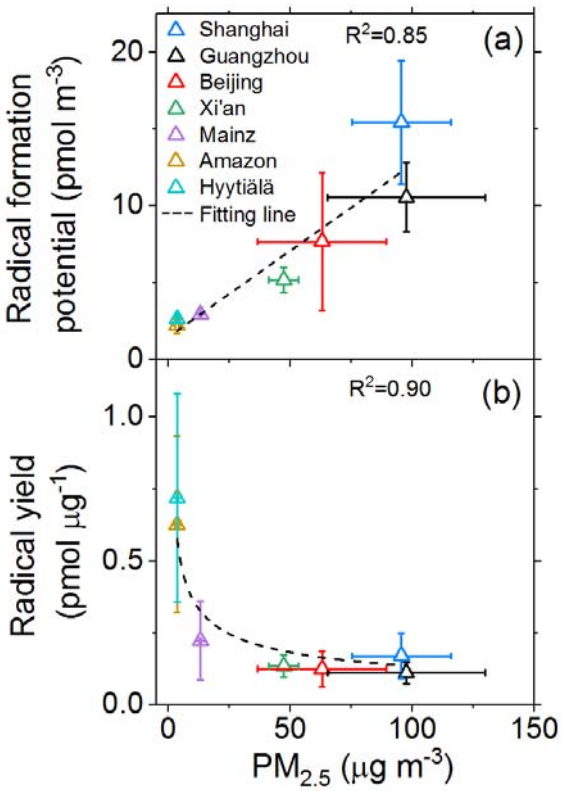

938

939 **Figure 5.** Correlation of air sample volume (a) and particle mass (b) normalized radical yields with

940 $PM_{2.5}$ concentrations. The error bars represent the standard deviation of measurements with more

941 than three individual samples.

942

943

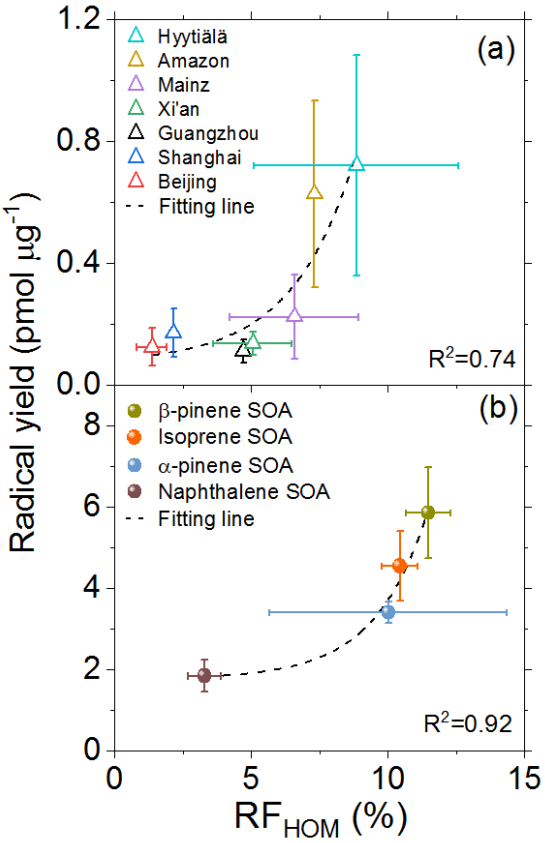

944
945 **Figure 6.** Correlation of particle mass normalized radical yield with relative ion number fraction
946 of HOMs associated with ambient fine PM (a) and laboratory SOA (b). The error bars represent
947 the standard deviation of measurement from replicates.
948

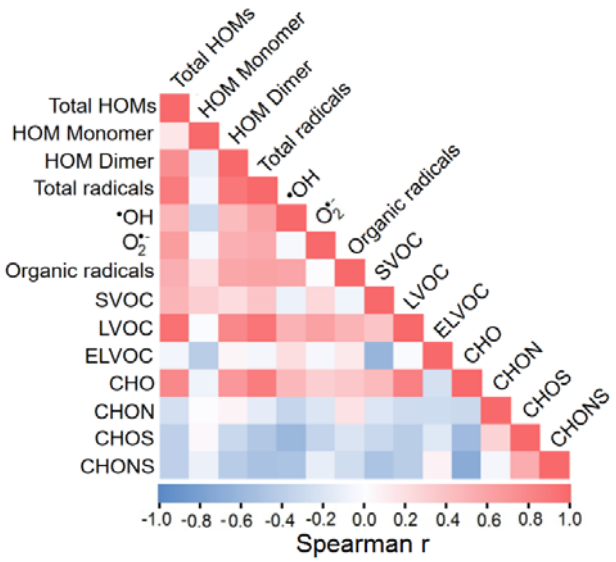

949

950 **Figure 7.** Spearman correlation matrix of HOM relative abundance and aerosol mass normalized

951 radical yield.

952

953 TOC/Abstract Art

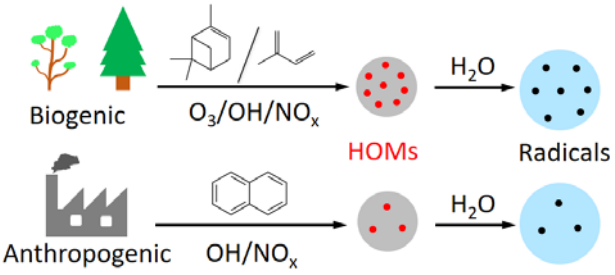

954

955